

One Pic is All it Takes: Poisoning Visual Document Retrieval Augmented Generation with a Single Image

Ezzeldin Shereen[†], Dan Ristea^{†‡}, Shae McFadden^{§†‡}, Burak Hasircioglu[†],
Vasilios Mavroudis[†], Chris Hicks[†]

[†]The Alan Turing Institute

[‡]University College London

[§]King's College London

Abstract

Multi-modal retrieval augmented generation (M-RAG) is instrumental for inhibiting hallucinations in large multi-modal models (LMMs) through the use of a factual knowledge base (KB). However, M-RAG introduces new attack vectors for adversaries that aim to disrupt the system by injecting malicious entries into the KB. In this paper, we present the first poisoning attack against M-RAG targeting visual document retrieval applications where the KB contains images of document pages. We propose two attacks, each of which require injecting only a single adversarial image into the KB. Firstly, we propose a universal attack that, for any potential user query, influences the response to cause a denial-of-service (DoS) in the M-RAG system. Secondly, we present a targeted attack against one or a group of user queries, with the goal of spreading targeted misinformation. For both attacks, we use a multi-objective gradient-based adversarial approach to craft the injected image while optimizing for both retrieval and generation. We evaluate our attacks against several visual document retrieval datasets, a diverse set of state-of-the-art retrievers (embedding models) and generators (LMMs), demonstrating the attack effectiveness in both the universal and targeted settings. We additionally present results including commonly used defenses, various attack hyper-parameter settings, ablations, and attack transferability.

1 Introduction

Large multi-modal models (LMMs) enable a wide range of zero-shot capabilities spanning a variety of input modalities, such as language, vision, and audio [1, 19]. However, similar to unimodal large language models (LLMs), they can suffer from hallucinations, generating outputs that are not grounded in factual information [11]. Retrieval augmented generation (RAG) [16] attempts to address this issue by retrieving trusted information chunks, that are relevant to the user query, directly from a knowledge base (KB). The retrieved information is then included in the input to the generative model to inform its generation.

The effectiveness of RAG relies primarily on the trustworthiness of the information in the KB. Challenging this assumption, recent work has shown that textual RAG pipelines are vulnerable to poisoning attacks, where an attacker injects malicious information into the KB [39, 32]. To create an impactful attack, the injected information must simultaneously (1) have a high chance of being retrieved, and (2) influence the output of the generative model. These attacks have recently been extended to multi-modal RAG (M-RAG) pipelines [4, 18] by concurrent research [9, 20].

Both concurrent works [9, 20] consider that user queries and KB consist of text-image pairs, thus the text modality is common between queries, KB items, and LMM outputs. This shared modality greatly simplifies the attack procedure. For instance, an adversary could simply inject the expected

user request alongside the malicious response into the KB [20]. This trivial-but-effective attack is not possible in many practical use cases such as visual document retrieval [7, 33] where the KB consists purely of images (document pages) and yet both the user queries and LMM outputs are textual. Therefore, it remains unclear whether M-RAG poisoning is still possible in the visual document-based setting.

In this paper, we bridge this gap in the literature by investigating poisoning attacks on visual document RAG (VD-RAG). We adapt projected gradient descent (PGD) [21] with a multi-objective loss, which we refer to as MO-PGD, to balance the optimization of the retrieval and generation objectives when crafting the malicious image. First, we propose a *universal attack* where the image is optimized to be retrieved and influence generation for all queries, thus causing a denial-of-service (DoS) attack against the VD-RAG pipeline. Second, we propose a stealthier *targeted attack* where the image only influences specific queries, thus causing targeted misinformation about a certain topic. In particular, we make the following contributions: (1) We propose the first poisoning attack against VD-RAG systems. (2) We demonstrate that our multi-objective PGD optimization approach allows an adversary to craft a single image that can either cause a DoS or targeted misinformation attacks against the VD-RAG pipeline. (3) Through extensive evaluations, we demonstrate various factors that contribute to the success of our attacks, including the models utilized and the attacks’ resilience against potential countermeasures. (4) Finally, we present an ablation of the ColPali embedding model, which demonstrated high robustness to our attacks.

2 Related Work

Multi-modal RAG. Early works on multi-modal RAG (M-RAG) [4] considered answering a textual question with the help of a KB consisting of image-text pairs. M-RAG has been shown to outperform single-modality RAG (text or vision) [25]. In addition, M-RAG has been applied in different domains, such as video retrieval [13], healthcare [30, 15], and autonomous driving [34].

Visual Document Retrieval. Building on the recent success of vision language models, visual document retrieval (VDR) attempts to utilize visual language models (VLMs) to create rich multi-modal representations of documents. The use of such representations has been shown to be more efficient than optical character recognition (OCR) pipelines on document retrieval benchmarks [7]. ColPali [7] proposed fine-tuning several VLMs to perform VDR using a late interaction based loss, inspired by ColBERT [14]. This concept was used for VD-RAG in [33], where it was shown to outperform textual RAG solutions based on OCR. Zhuang et al. [38] investigated the vulnerability of document retrievers to adversarial attacks; however, the work did not consider the joint problem of retrieval and generation.

Attacks on Textual RAG. The first data poisoning attack proposed against textual RAG pipelines was PoisonedRAG [39], which divides the injected malicious document into two parts to optimize each objective (retrieval and generation) separately. A similar approach was also proposed by [32, 26]. However, most of these approaches handle the retrieval objective by using the query string and gradient-based or word-swapping-based attacks to optimize for generation.

Attacks on Multi-modal RAG. Recent works have started extending the above attacks to the multimodal domain and thus are the most similar to our work. Ha et al. [9] proposed targeted and universal poisoning attacks against multi-modal RAG systems. Shortly after, Liu et al. [20] proposed a targeted misinformation poisoning attack against a multi-modal RAG system. Importantly, these works consider KBs including image-text pairs, greatly simplifying the attacks. Furthermore, the targeted multi-modal embedding models in these works are typically outdated and include known vulnerabilities, as a result of the so-called modality gap [17]. Moreover, these recent works did not consider the resilience of their attacks to potential defenses. Our work specifically targets VD-RAG pipelines, where the attacker cannot manipulate text, thus making a novel contribution to the field of RAG poisoning.

Defenses against RAG Poisoning. Due to the recency of the field, the literature still lacks specific defenses against multi-modal RAG poisoning, let alone VD-RAG. Therefore, we leverage the most common defenses against textual RAG poisoning attacks. The works proposing RAG poisoning attacks [39, 26] evaluated their proposed attacks against defenses, including (1) knowledge expansion

(increasing the number of context documents retrieved), (2) paraphrasing the user query, and (3) filtering out suspicious textual documents with high perplexity. Furthermore, LLM-as-a-judge frameworks could be used to evaluate and detect RAG poisoning [36, 3]. Other works proposed specific approaches to defend against RAG poisoning. For example, RobustRAG [31] proposed a certifiably robust isolate-then-aggregate framework, where an answer is generated using each retrieved document separately, and then the answers are aggregated based on the most common keywords in the isolated answers, or based on averaging the next token probabilities. Moreover, [37] proposed TrustRAG, a two-stage framework to detect RAG poisoning when the attacker can control a substantial amount of documents: (1) document filtering based on K-means clustering and ROUGE metric, and (2) consolidation between the knowledge retrieved and the internal knowledge of the LLM. Despite the demonstrated success of [31] and [37] in mitigating attacks, they report significant drops in performance on benign data.

3 VD-RAG Pipeline

A visual document RAG pipeline consists of three main components. First, a *knowledge base* (KB) $\mathcal{K} = \{I_1, \dots, I_K\}$ containing a set of K images, each corresponding to a page in a document. Second, a *retriever* \mathcal{R} uses a multi-modal embedding model $E(\cdot)$ that projects user queries (text) and KB images into a common vector space. The retriever then computes a similarity score $S(E(q), E(I))$ between a user query q and each image in $I \in \mathcal{K}$. Common similarity metrics for RAG retrievers include cosine similarity and *MaxSim* proposed in [7]. For each user query q , the retriever retrieves the top- k relevant items from \mathcal{K} according to the similarity score, where $k \ll |\mathcal{K}|$. Formally, the retriever computes $R(q, \mathcal{K}) = \text{top-}k_{I \in \mathcal{K}} S(E(q), E(I))$. The third component is a *generator* \mathcal{G} which is a vision language model (VLM) used to generate a response g to the user’s query q with the retrieved images in its context window. That is, $g = \mathcal{G}(q, R(q, \mathcal{K}))$.

4 Poisoning Attacks against VD-RAG

Threat Model. We consider an attacker that aims to disrupt the operation of the visual document RAG system by causing the retriever to retrieve the adversarial image and the generator to generate unhelpful responses to user queries. To achieve this goal, the attacker is assumed to have a dataset of potential user queries \mathcal{Q} , ground truth answers \mathcal{A} , and KB images \mathcal{I} from the same distribution as in the attacked RAG system. Furthermore, the attacker is capable of injecting documents/images into the KB. This could be realized either by an insider that has access to inject and modify enterprise-owned documents, or by an outsider injecting the poisoned documents/images in public domains (KBs are typically crawled from the internet, such as from Wikipedia [20]). In our work, we assume a weak attacker that can inject only one malicious image I' into the KB s.t. $\mathcal{K}' = \mathcal{K} \cup I'$.

The injected image is used to realize one of two malicious objectives: (1) a *universal attack* where the injected image should be both retrieved and influence generation for any possible user query, and (2) a *targeted attack* where the image should only be retrieved and influence generation for a specific query or a subset of related queries. While the first attack corresponds to a denial-of-service (DoS) attack against the availability of the VD-RAG system, the second attack corresponds to more stealthy and specific objectives, such as spreading misinformation on specific topics.

We examine both the *white-box* and the *black-box* settings. In the white-box setting, the attacker is assumed to have knowledge of both the embedding model and the VLM. This is motivated by the vast amount of competent open-source text and multi-modal embedding models [7], as well as VLMs [5]. In the black-box setting, we consider that the attacker uses models other than those used in the VD-RAG system to craft the malicious image, and we consequently evaluate the transferability between adversarial samples from one model to another.

Proposed Attack. We present an overview of our attack in Figure 1. Building upon the work of [39], a successful RAG poisoning attack must meet two conditions. First, the *retrieval condition* requires that the malicious image is retrieved for the attacker-specified queries. Second, the *generation condition* requires that when present in the context window, the malicious image must cause the generator to generate a specific response.

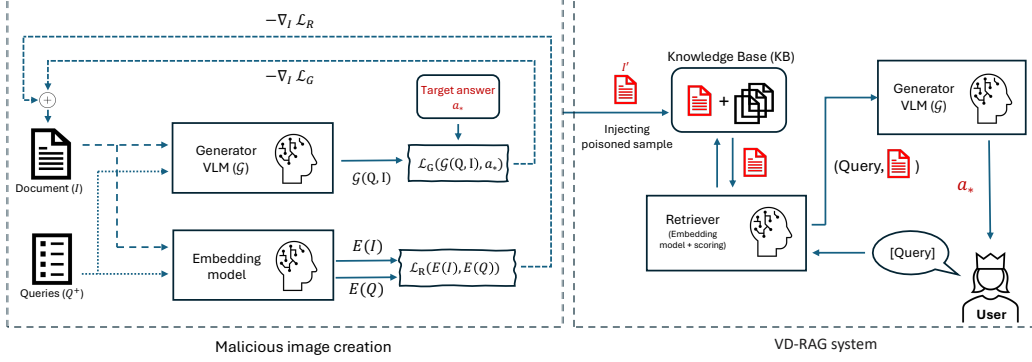


Figure 1: Overview of our attack. We select an arbitrary document/image I and optimize it against target queries Q^+ in the training set (shown on the left). The resulting poisoned document I' is then injected into the KB. When the attack is successful, I' is retrieved and causes the generator G to malfunction (shown on the right).

In order to compute a malicious image I' that meets the above two conditions, we adopt a gradient-based adversarial example framework, initially proposed against neural network-based image classifiers [8, 2, 21]. In particular, we extend PGD to jointly optimize the image to minimize a multi-objective loss function \mathcal{L}_{RAG} capturing both a retrieval loss \mathcal{L}_R and a generation loss \mathcal{L}_G as follows

$$\mathcal{L}_{RAG} = \lambda_R \mathcal{L}_R + \lambda_G \mathcal{L}_G, \quad (1)$$

where λ_R, λ_G are attacker-chosen coefficients.

For the *targeted* attack, the adversary chooses a subset of positive target queries $Q^+ \subset Q$ that it wishes to influence, and the remaining queries $Q^- = Q / Q^+$ are referred to as negative queries. The answers \mathcal{A} are divided, respectively. The retrieval and generation losses are defined as follows.

$$\mathcal{L}_R = \sum_{i=1}^{|Q^+|} (1 - S(q_i, I')) - \sum_{i=1}^{|Q^-|} (1 - S(q_i, I')), \quad (2)$$

$$\mathcal{L}_G = \sum_{i=1}^{|Q|} CE(\mathcal{G}(q_i, \mathcal{I}_{k-1} \cup I'), a_i^*), \quad (3)$$

where $CE(\cdot)$ is the cross entropy loss, \mathcal{I}_{k-1} is a randomly sampled subset (with cardinality $|\mathcal{I}_{k-1}| = k - 1$) of the attacker-owned KB image dataset \mathcal{I} , a_i^* is the desired target answer by the attacker for query $q_i \in Q^+$ and the ground truth answer for query $q_i \in Q^-$. Note that $\mathcal{I}_{k-1} \cup I'$ represents the top- k retrieved images simulated by the attacker.

Note that the *universal* attack can be considered as a special case of the targeted attack where $Q^+ = Q$.

5 Experiment Design

Datasets. We evaluate our attacks on two visual document retrieval datasets taken from the ViDoRe benchmark versions 1 and 2. In particular, we use the datasets `syntheticDocQA_artificial_intelligence_test` (which will be referred to as ViDoRe-V1-AI for short moving forward) and `restaurant_esg_reports_beir` (which we will refer to as ViDoRe-V2-ESG) [7]. ViDoRe-V1-AI consists of 100 queries and 1000 images (with exactly one relevant ground-truth image in the KB per query), while ViDoRe-V2-ESG consists of 52 queries and 1538 images with an average of 2.5 relevant images per query¹. We split the queries of each dataset into a training set (80%, used to optimize the malicious image) and a test set (20%). For KB images, we assume that the attacker knows 10% of the images in each dataset, that is, $|\mathcal{I}| = 0.1|\mathcal{K}|$.

¹Not all images in the KB have to be relevant for a query.

Embedding Models. We use a mix of embedding models that range in their sizes, recency, and target applications: (1) CLIP-ViT-LARGE is a seminal multi-modal 0.4B parameter model proposed in [24] trained using contrastive learning to achieve zero-shot image classification. (2) GME-Qwen2-VL-2B is a 2.2B parameter model [35] fine-tuned from Qwen2-2B-VL on several tasks, including VDR. (3) ColPali-v1.3 is a state-of-the-art 3B parameter model [7] in visual document retrieval, using ColBERT-style [14] late embedding interaction, and incorporating the retrieval similarity metric *MaxSim*. For the above models, unless otherwise stated, we assume that the retriever only retrieves the top-1 relevant image from the KB.

VLMs. We evaluate our attacks on two VLMs: SmolVLM-Instruct (2.2B) [22] and Qwen2.5-VL-3B-Instruct (3.75B) [29]. At the time of writing, these models ranked 25th and 5th in the OpenCompass VLM leaderboard [6] for open-source models with less than 4B parameters.

Defenses. The literature lacks specialized defenses against multi-modal RAG poisoning attacks. Furthermore, most of the defenses proposed for textual RAG are not straightforwardly applicable to multi-modal settings and incur a significant drop in benign performance [31, 37]. Nevertheless, we evaluate the resistance of our attacks to several approaches that are commonly-used to increase the trustworthiness of RAG systems, which have been used by previous works as defenses. These include:

- (1) **Knowledge expansion:** This defense works by retrieving a larger number of KB items with the intention of diluting the effect of the retrieved adversarial image and was used as a defense in [39]. We consider expanding the number of retrieved images from 1 to 5 images.
- (2) **VLM-as-a-judge:** We use a VLM-as-a-Judge [3, 36] to evaluate the output on three metrics: (i) *answer relevancy* to assess whether the answer is relevant to the query, (ii) *context relevancy* to assess if the retrieved images are relevant to the query, and (iii) *answer faithfulness* to assess if the answer is grounded in the retrieved images. We used an adapted version of the prompts used in [25] (found in G) and use the same models used as VLMs.
- (3) **Query Paraphrasing:** As previously used by [26], we asked a SoTA LLM (in our case, Llama-3.1-8B-Instruct) to paraphrase all queries in the ViDoRe-V1-AI and ViDoRe-V2-ESG datasets, and used them to evaluate whether attacks are still successful.

Baselines. We compare our attacks to naively prompting a state-of-the-art LLM (GPT4o [12]) to generate an adversarial image. This approach has been utilized by previous works proposing attacks against textual (where the LLM generates text KB items) [39, 26] and multi-modal RAG [9, 20].

Evaluation Metrics. We evaluate the RAG system and the attack using the following performance metrics: 1) Recall-B is the fraction of queries for which \mathcal{R} retrieves a relevant image prior to attack; 2) Recall-A is the fraction of queries for which \mathcal{R} retrieves a relevant image after the attack (lower is better for the adversary); 3) SIM-G-GT is the average embedding similarity between the VLM generated response for targeted queries and the ground truth response, computed using the Jina-Embeddings-V3 [28] text embedding model (lower is better for the adversary); 4) ASR-R is the fraction of targeted queries for which the malicious image is retrieved by \mathcal{R} (higher is better for the adversary); 5) ASR-G-Hard is the fraction of targeted queries for which the VLM outputs the target response a_i^* verbatim (higher is better); 6) SIM-G-ADV-POS is the average embedding similarity between the VLM generated response for targeted queries and the target response, computed similar to SIM-G-GT (higher is better); 7) FPR-R is the fraction of non-targeted queries for which the malicious image is retrieved by \mathcal{R} (lower is better); 8) SIM-G-ADV-NEG is the average embedding similarity between the VLM generated response for non-targeted queries and the target response, computed similar to SIM-G-GT (lower is better). For all evaluation metrics the suffix "@k" signifies that the metric is reported when the top- k relevant images are retrieved. Furthermore, to separate the generation performance from retrieval, we report the metrics "@-1" which means that we force our malicious image to be retrieved as the only context image.

Attack Hyper-parameters. For each considered dataset, we pick an arbitrary image that is not relevant to any query, to act as a starting point for our optimization process. We produced our attacks through projected gradient descent (PGD) [21] using a linear learning rate schedule from 3×10^{-3} to 3×10^{-4} over 500 gradient steps with a batch size of 8 user queries, $\lambda_R = 2$, $\lambda_G = 1$ and a maximum

image perturbation $\alpha = \frac{8}{255}$. This choice was made based on our study of different perturbation budgets in Appendix C. The retrieval loss uses the cosine similarity between embeddings as $S(q, I)$, while the generation loss for the universal attack uses the target malicious reply: I will not reply to you!.

Compute Resources and Code. The experiments were carried out on a NVIDIA H100 NVL GPU with 93GiB VRAM. The code used to run the experiments, including all configurations, and their results is available at [27].

6 Universal Attack

This section presents the results for the universal attack and discusses the vulnerability of the different embedding models and VLMs to the attack.

Table 1: Retrieval and generation performance of the universal attack under different embedding models and VLMs.

Attack Type	Eval Embedder	Eval VLM	Recall-B @1	Recall-A @1	ASR-R @1	Recall-B @5	Recall-A @5	ASR-R @5	ASR-G-Hard	SIM-G-ADV-POS	SIM-G-GT
Our Attack	CLIP-L	SmolVLM	0.210	0.020	1.000	0.440	0.430	1.000	1.000	1.000	0.030
		Qwen2.5-3B	0.210	0.010	1.000	0.440	0.430	1.000	1.000	1.000	0.030
	ColPali	SmolVLM	0.660	0.650	0.000	0.980	0.980	0.100	0.050	0.053	0.488
		Qwen2.5-3B	0.660	0.660	0.000	0.980	0.980	0.100	1.000	1.000	0.030
	GME	SmolVLM	0.580	0.580	0.000	0.940	0.930	0.250	1.000	1.000	0.030
		Qwen2.5-3B	0.580	0.580	0.000	0.940	0.930	0.350	1.000	1.000	0.030
	CLIP-L	SmolVLM	0.210	0.210	0.000	0.440	0.440	0.000	0.000	-0.024	0.550
		Qwen2.5-3B	0.210	0.210	0.000	0.440	0.440	0.000	0.000	0.014	0.529
GPT Attack	ColPali	SmolVLM	0.660	0.650	0.000	0.980	0.980	0.000	0.000	-0.004	0.515
		Qwen2.5-3B	0.660	0.650	0.000	0.980	0.980	0.000	0.000	0.005	0.544
	GME	SmolVLM	0.580	0.580	0.000	0.940	0.940	0.000	0.000	-0.023	0.533
		Qwen2.5-3B	0.580	0.580	0.000	0.940	0.940	0.000	0.000	0.019	0.512

Attack Performance. Table 1 presents an evaluation of our universal attack on the ViDoRe-V1-AI dataset, shown for the embedding models and VLMs considered. Results for the ViDoRe-V2-ESG dataset are presented in Appendix B. For retrieval, the universal attack produces an image that is always retrieved (ASR-R @1) for all queries when the CLIP-ViT-LARGE embedding model is used. To the contrary, state-of-the-art embedding models (ColPali-v1.3 and GME-Qwen2-VL-2B) never retrieve the adversarial image retrieved image as the top-1 relevant image, but sometimes retrieve it within the top-5. Regarding generation, the universal attack consistently causes SmolVLM-Instruct and Qwen2.5-VL-3B-Instruct to generate the target answer *verbatim* for almost all user queries in the test dataset. For both retrieval and generation, we observe that our attack is clearly outperforming the GPT-4o based baseline.

Black-Box Transferability. The results in Table 1 show that, in a white-box, the universal attack is successful against CLIP-ViT-LARGE for retrieval and SmolVLM-Instruct as well as Qwen2.5-VL-3B-Instruct for generation. We additionally evaluated the universal attack in a black-box setting, where the adversary does not have access to the embedding model and VLM used in the RAG system (see Appendix D). We did not observe any transferability of the attack across the different embedding and VLM models.

Multi-Model Generalization. Motivated by the poor black-box transferability of the attack, we attempt to optimize an adversarial image against all considered embedding and VLM models. Subsequently, we evaluated the performance of the generated image against each pair of embedding and VLM models. We considered two multi-model attacks [10]: (i) an attack trained on the CLIP-ViT-LARGE and GME-Qwen2-VL-2B embedding models as well as all VLMs (i.e., 2x2), and (ii) an attack trained on all embedding models and VLMs (i.e., 3x2). The results in Table 14 (Appendix F) show that the attack is capable of generalizing across VLMs for generation, while it is harder to generalize for retrieval (especially for the 3x2 attack). Notably, ColPali-v1.3 and GME-Qwen2-VL-2B remain robust to influences under all attacks.

Investigation of the Robustness of SoTA Embedding Models. In Appendix E, we provide UMAP visualizations [23] of the queries and images in each embedding space. The UMAP visualizations show a distinct modality gap in CLIP-ViT-LARGE, however, a minimal gap for ColPali-v1.3 and GME-Qwen2-VL-2B. This illustrates the difficulty in generating a single image to be retrieved for all queries in these embedding spaces, which leads to their observed robustness.

To further investigate the origin of this phenomenon, we performed ablations on ASR-R @1 metric of ColPali w.r.t. to dimensions: the similarity metric used for retrieval and whether the model is prompted by text and image or only the images. We consider 4 losses: *MaxSim*, which is the original metric used by ColPali, *AvgSim*, which replaces the max operator by the average, *SoftMaxSim*, which replaces the max operator by softmax, and *CosAvg*, which computes the cosine similarity of the averaged token embeddings for both queries and images. Additional information about the MaxSim metric can be found in Appendix E. Table 2 shows the ablation results and shows that the loss function used is partly responsible for the robustness of ColPali.

Table 2: Ablation results of the robustness of ColPali (ASR-R @1) to universal VD-RAG poisoning attacks.

Context Type	MaxSim	AvgSim	SoftMaxSim	CosAvg
Image + Text	0.000	0.250	0.150	0.050
Image Only	0.000	0.250	0.050	0.050

7 Targeted Attack

As a result of the reduced modality gap in the embedding space of ColPali-v1.3 and GME-Qwen2-VL-2B, we investigate a more constrained single image attack that targets a fewer number of queries. We consider three targeted settings:

Setting I: Targeting One Query. In this setting, we consider targeting the first query in the dataset to generate a malicious answer generated by GPT-4o. The results for Setting I, seen in Table 3, show successful retrieval and generation manipulation across all embedding and VLM models. It also shows that despite the success of the GPT attack in this setting, our attacks still produces answers that are closer to the targeted malicious answers (as shown by SIM-G-ADV-POS).

Table 3: Performance of the targeted attacks against a single query (Setting I).

Attack Type	Embedder	VLM	ASR-R (@1)	FPR-R (@1)	SIM-G-ADV-POS	SIM-G-ADV-NEG
Our Attack	CLIP-L	SmolVLM	1.000	0.000	0.979	0.233
		Qwen2.5-3B	1.000	0.000	1.000	0.234
	ColPali	SmolVLM	1.000	0.000	1.000	0.239
		Qwen2.5-3B	1.000	0.000	1.000	0.225
	GME	SmolVLM	1.000	0.000	1.000	0.199
		Qwen2.5-3B	1.000	0.000	1.000	0.254
GPT Attack	CLIP-L	SmolVLM	1.000	0.000	0.793	0.271
		Qwen2.5-3B	1.000	0.000	0.895	0.222
	ColPali	SmolVLM	1.000	0.000	1.000	0.341
		Qwen2.5-3B	1.000	0.000	0.966	0.234
	GME	SmolVLM	1.000	0.000	0.966	0.303
		Qwen2.5-3B	1.000	0.000	0.929	0.246

Black-Box Transferability. The black-box transferability of the targeted one query attack is also investigated and the multi-model attack is trained as with the universal attack. These results, shown in Appendix D, demonstrate a similar lack of black-box transferability between different models.

Multi-Model Generalization. We perform the same multi-model evaluation as with the universal attack. Appendix F shows a near perfect generalization of targeted attack images for both retrieval and generation. Except in the case where ColPali-v1.3 is included in the training set, which has an adverse impact on the GME-Qwen2-VL-2B results.

Setting II: Targeting Multiple Queries. The multiple target subvariant of the targeted attack optimizes the image to be retrieved and influence generation for a cluster of queries. When the image is retrieved, the VLM should generate the same answer for all of them. Therefore, the attack acts as an intermediate step between the base targeted attack and the universal attack. We consider targeting 5 queries (query 1 in the dataset, as well as its 4 nearest neighbors, computed by the Jina-Embeddings-V3 [28] model). Table 4 shows that despite the inability of the universal attack to

Table 4: Performance of the targeted attacks against a cluster of queries (Setting II). Results only for SmolVLM.

Attack Type	Embedder	ASR-R (@1)	FPR-R (@1)	SIM-G-ADV-POS	SIM-G-ADV-NEG
Our Attack	CLIP-L	1.000	0.000	1.000	0.174
	ColPali	1.000	0.000	0.098	0.005
	GME	0.600	0.000	1.000	0.028
GPT Attack	CLIP-L	0.400	0.000	-0.016	0.016
	ColPali	0.400	0.000	-0.023	-0.015
	GME	0.200	0.000	0.004	-0.026

influence retrieval for ColPali-v1.3 and GME-Qwen2-VL-2B, the multiple-target variant is able to influence retrieval for five and three targeted queries out of five, respectively.

Setting III: Targeting Multiple Queries & Answers. In this setting, the attack targets multiple queries with the intent of generating a different malicious answer for each query. we consider queries 1 and 2 in the datasets with malicious answers generated by GPT-4o. Table 5 shows similar results to the attack in Setting II, where our attack can be successful against both legacy and SoTA embedding models. Moreover, our attack still demonstrates clear superiority to the GPT-4o baseline.

Table 5: Performance of the targeted attacks against multiple queries and multiple answers (Setting III). Results only for SmolVLM.

Attack Type	Embedder	ASR-R (@1)	FPR-R (@1)	SIM-G-ADV-POS	SIM-G-ADV-NEG
Our Attack	CLIP-L	1.000	0.000	1.000	0.270
	ColPali	1.000	0.000	0.527	0.260
	GME	0.500	0.000	1.000	0.263
GPT Attack	CLIP-L	0.500	0.000	0.671	0.321
	ColPali	0.000	0.000	0.728	0.313
	GME	0.500	0.000	0.847	0.310

8 Defenses

Knowledge Expansion. Tables 6 and 7 show the attack performance under different numbers of retrieved images (1 or 5). The table rows show the top-k that was used during training the attack. The results show that expanding the retrieved knowledge (using $k = 5$) can degrade the attack’s performance. However, an adaptive attack trained specifically against this value of k (i.e., the second row in both tables) can effectively evade this defense. Therefore, we conclude that knowledge expansion on its own cannot guarantee the robustness of the RAG system against our attacks.

Table 6: Universal attack when applying the knowledge expansion defense (increasing k from 1 to 5). Results for CLIP-L and SmolVLM.

Attack Top- k	ASR-G-Hard (@1)	SIM-G-ADV-POS (@1)	ASR-G-Hard (@5)	SIM-G-ADV-POS (@5)
1	0.950	0.948	0.000	-0.029
5	0.950	0.946	1.000	1.000

VLM-as-a-Judge. Table 8 reports the performance of using the VLMs (SmolVLM and Qwen2.5-3B) as a judge. Qwen2.5-3B-as-a-judge demonstrates the capability to detect both the universal and targeted attacks across all three metrics. SmolVLM-as-a-judge detects low answer relevancy for both attacks but performs worse in the other two metrics. Additionally, SmolVLM is better able to detect the universal attack than the targeted attack. Table 9 reports the performance of judge performance after the attack had been trained with the loss of the judge included. The results show that adaptive attacks trained against the judge are able to bypass the defense but there is no transferability between judge models.

Table 7: Targeted attack (Setting I) when applying the knowledge expansion defense (increasing k from 1 to 5). Results for CLIP-L and SmolVLM.

Attack Top- k	SIM-G-ADV-POS (@1)	SIM-G-ADV-NEG (@1)	SIM-G-ADV-POS (@5)	SIM-G-ADV-NEG (@5)
1	1.000	-0.014	-0.065	-0.025
5	1.000	-0.018	1.000	-0.027

Table 8: VLM-as-a-Judge evaluation scores for non-targeted and targeted attacks, judged by different VLMs.

Attack Type	Embedder	Eval Judge	Image Content Relevancy	Image Faithfulness	Answer Relevancy
Non-targeted	CLIP-L	SmolVLM	0.550	0.300	0.000
		Qwen2.5-3B	0.000	0.000	0.000
Targeted	CLIP-L	SmolVLM	0.650	0.750	0.200
		Qwen2.5-3B	0.000	0.000	0.000

Table 9: Adaptive attacks against judge: Evaluation of image relevance, faithfulness, and answer quality under non-targeted and targeted settings, using different judge/eval judge combinations.

Attack Type	Judge	Eval Judge	Image Content Relevancy	Image Faithfulness	Answer Relevancy
Non-targeted	SmolVLM	SmolVLM	1.000	1.000	1.000
	SmolVLM	Qwen2.5-3B	0.000	0.000	0.000
	Qwen2.5-3B	SmolVLM	0.450	0.050	0.050
	Qwen2.5-3B	Qwen2.5-3B	1.000	1.000	1.000
Targeted	SmolVLM	SmolVLM	1.000	1.000	1.000
	SmolVLM	Qwen2.5-3B	0.050	0.000	0.000
	Qwen2.5-3B	SmolVLM	0.750	0.650	0.000
	Qwen2.5-3B	Qwen2.5-3B	1.000	1.000	1.000

Query Paraphrasing. Our results shows that query paraphrasing is not an effective defense against our attacks (computed against the original queries). In the universal setting, our attacks achieved ASR-R and ASR-G-Hard of 0.95 after all queries were paraphrased. In the targeted setting, the ASR-R and SIM-G-ADV-POS stayed at exactly 1 after applying the defense.

9 Conclusion

In this paper, we demonstrate the first poisoning attacks against VD-RAG systems. Our attack showcased that conventional embedding models and VLMs are vulnerable to adversarial perturbation, where a single injected image is capable of either causing a DoS in the entire RAG pipeline (both retrieval and generation) or spreading misinformation on targeted topics. We also observed the notable adversarial robustness of the ColPali-v1.3 and GME-Qwen2-VL-2B embedding models under the universal attack case; however, they still proved vulnerable to more targeted attacks. Beyond a base VD-RAG pipeline, our results also demonstrated that commonly used RAG defenses are insufficient in defending VD-RAG from poisoning. Our aim is that the proposed universal and targeted attacks provide the first step toward understanding the vulnerability of visual document RAG systems and enhancing their robustness for future adoption.

References

- [1] Florian Bordes, Richard Yuanzhe Pang, Anurag Ajay, Alexander C Li, Adrien Bardes, Suzanne Petryk, Oscar Mañas, Zhiqiu Lin, Anas Mahmoud, Bargav Jayaraman, et al. An introduction to vision-language modeling. *arXiv preprint arXiv:2405.17247*, 2024.
- [2] Nicholas Carlini and David Wagner. Towards evaluating the robustness of neural networks. In *2017 IEEE Symposium on Security and Privacy (SP)*, pages 39–57. Ieee, 2017.
- [3] Dongping Chen, Ruoxi Chen, Shilin Zhang, Yaochen Wang, Yinuo Liu, Huichi Zhou, Qihui Zhang, Yao Wan, Pan Zhou, and Lichao Sun. Mllm-as-a-judge: Assessing multimodal llm-as-a-judge with vision-language benchmark. In *Forty-first International Conference on Machine Learning*, 2024.
- [4] Wenhui Chen, Hexiang Hu, Xi Chen, Pat Verga, and William Cohen. MuRAG: Multimodal retrieval-augmented generator for open question answering over images and text. In *Proceedings of the 2022 Conference on Empirical Methods in Natural Language Processing*, pages 5558–5570, 2022.
- [5] Haodong Duan, Junming Yang, Yuxuan Qiao, Xinyu Fang, Lin Chen, Yuan Liu, Xiaoyi Dong, Yuhang Zang, Pan Zhang, Jiaqi Wang, et al. Vlmevalkit: An open-source toolkit for evaluating large multi-modality models. In *Proceedings of the 32nd ACM International Conference on Multimedia*, pages 11198–11201, 2024.
- [6] Haodong Duan, Junming Yang, Yuxuan Qiao, Xinyu Fang, Lin Chen, Yuan Liu, Xiaoyi Dong, Yuhang Zang, Pan Zhang, Jiaqi Wang, et al. Vlmevalkit: An open-source toolkit for evaluating large multi-modality models. In *Proceedings of the 32nd ACM international conference on multimedia*, pages 11198–11201, 2024.
- [7] Manuel Faysse, Hugues Sibille, Tony Wu, Bilel Omrani, Gautier Viaud, Céline Hudelot, and Pierre Colombo. Colpali: Efficient document retrieval with vision language models. In *The Thirteenth International Conference on Learning Representations*, 2024. Colpali-v1.3 model source <https://huggingface.co/vidore/colpali-v1.3>. ViDoRe-V1-AI dataset source https://huggingface.co/datasets/vidore/syntheticDocQA_artificial_intelligence_test. ViDoRe-V2-ESG dataset source https://huggingface.co/datasets/vidore/restaurant_esg_reports_beir.
- [8] Ian J Goodfellow, Jonathon Shlens, and Christian Szegedy. Explaining and harnessing adversarial examples. *arXiv preprint arXiv:1412.6572*, 2014.
- [9] Hyeonjeong Ha, Qiusi Zhan, Jeonghwan Kim, Dimitrios Bralios, Saikrishna Sanniboina, Nanyun Peng, Kai-wei Chang, Daniel Kang, and Heng Ji. MM-PoisonRAG: Disrupting multimodal rag with local and global poisoning attacks. *arXiv preprint arXiv:2502.17832*, 2025.
- [10] Xiao Hu, Eric Liu, Weizhou Wang, Xiangyu Guo, and David Lie. MARAGE: Transferable multi-model adversarial attack for retrieval-augmented generation data extraction. *arXiv preprint arXiv:2502.04360*, 2025.
- [11] Lei Huang, Weijiang Yu, Weitao Ma, Weihong Zhong, Zhangyin Feng, Haotian Wang, Qianglong Chen, Weihua Peng, Xiaocheng Feng, Bing Qin, et al. A survey on hallucination in large language models: Principles, taxonomy, challenges, and open questions. *ACM Transactions on Information Systems*, 43(2):1–55, 2025.
- [12] Aaron Hurst, Adam Lerer, Adam P Goucher, Adam Perelman, Aditya Ramesh, Aidan Clark, AJ Ostrow, Akila Welihinda, Alan Hayes, Alec Radford, et al. Gpt-4o system card. *arXiv preprint arXiv:2410.21276*, 2024.
- [13] Soyeong Jeong, Kangsan Kim, Jinheon Baek, and Sung Ju Hwang. Videorag: Retrieval-augmented generation over video corpus. *arXiv preprint arXiv:2501.05874*, 2025.
- [14] Omar Khattab and Matei Zaharia. Colbert: Efficient and effective passage search via contextualized late interaction over bert. In *Proceedings of the 43rd International ACM SIGIR conference on research and development in Information Retrieval*, pages 39–48, 2020.

- [15] Aritra Kumar Lahiri and Qinmin Vivian Hu. Alzhemerrag: Multimodal retrieval augmented generation for pubmed articles. *arXiv preprint arXiv:2412.16701*, 2024.
- [16] Patrick Lewis, Ethan Perez, Aleksandra Piktus, Fabio Petroni, Vladimir Karpukhin, Naman Goyal, Heinrich Küttler, Mike Lewis, Wen-tau Yih, Tim Rocktäschel, et al. Retrieval-augmented generation for knowledge-intensive nlp tasks. *Advances in neural information processing systems*, 33:9459–9474, 2020.
- [17] Victor Weixin Liang, Yuhui Zhang, Yongchan Kwon, Serena Yeung, and James Y Zou. Mind the gap: Understanding the modality gap in multi-modal contrastive representation learning. *Advances in Neural Information Processing Systems*, 35:17612–17625, 2022.
- [18] Weizhe Lin and Bill Byrne. Retrieval augmented visual question answering with outside knowledge. In *Proceedings of the 2022 Conference on Empirical Methods in Natural Language Processing*, pages 11238–11254, 2022.
- [19] Haotian Liu, Chunyuan Li, Qingyang Wu, and Yong Jae Lee. Visual instruction tuning. *Advances in neural information processing systems*, 36:34892–34916, 2023.
- [20] Yinuo Liu, Zenghui Yuan, Guiyao Tie, Jiawen Shi, Lichao Sun, and Neil Zhenqiang Gong. Poisoned-MRAG: Knowledge poisoning attacks to multimodal retrieval augmented generation. *arXiv preprint arXiv:2503.06254*, 2025.
- [21] Aleksander Madry, Aleksandar Makelov, Ludwig Schmidt, Dimitris Tsipras, and Adrian Vladu. Towards deep learning models resistant to adversarial attacks. *arXiv preprint arXiv:1706.06083*, 2017.
- [22] Andrés Marafioti, Orr Zohar, Miquel Farré, Merve Noyan, Elie Bakouch, Pedro Cuenca, Cyril Zakka, Loubna Ben Allal, Anton Lozhkov, Nouamane Tazi, Vaibhav Srivastav, Joshua Lochner, Hugo Larcher, Mathieu Morlon, Lewis Tunstall, Leandro von Werra, and Thomas Wolf. SmolVLM: Redefining small and efficient multimodal models. SmolVLM-Instruct source <https://huggingface.co/HuggingFaceTB/SmolVLM-Instruct>., 2025.
- [23] Leland McInnes, John Healy, and James Melville. UMAP: Uniform manifold approximation and projection for dimension reduction. *arXiv preprint arXiv:1802.03426*, 2018.
- [24] Alec Radford, Jong Wook Kim, Chris Hallacy, Aditya Ramesh, Gabriel Goh, Sandhini Agarwal, Girish Sastry, Amanda Askell, Pamela Mishkin, Jack Clark, et al. Learning transferable visual models from natural language supervision. In *International conference on machine learning*, pages 8748–8763. PmlR, 2021. Clip-ViT-LARGE source <https://huggingface.co/openai/clip-vit-large-patch14>.
- [25] Monica Riedler and Stefan Langer. Beyond text: Optimizing RAG with multimodal inputs for industrial applications. *arXiv preprint arXiv:2410.21943*, 2024.
- [26] Avital Shafran, Roei Schuster, and Vitaly Shmatikov. Machine against the RAG: Jamming retrieval-augmented generation with blocker documents. *arXiv preprint arXiv:2406.05870*, 2024.
- [27] Ezzeldin Shereen, Dan Ristea, Shae McFadden, and Burak Hasircioglu. MuMoRAG-attacks, 2025. URL <https://github.com/alan-turing-institute/mumORAG-attacks/>.
- [28] Saba Sturua, Isabelle Mohr, Mohammad Kalim Akram, Michael Günther, Bo Wang, Markus Krimmel, Feng Wang, Georgios Mastrapas, Andreas Koukounas, Andreas Koukounas, Nan Wang, and Han Xiao. jina-embeddings-v3: Multilingual embeddings with task lora, 2024. URL <https://arxiv.org/abs/2409.10173>. Jina-Embeddings-V3 source <https://huggingface.co/jinaai/jina-embeddings-v3>.
- [29] Peng Wang, Shuai Bai, Sinan Tan, Shijie Wang, Zhihao Fan, Jinze Bai, Keqin Chen, Xuejing Liu, Jialin Wang, Wenbin Ge, Yang Fan, Kai Dang, Mengfei Du, Xuancheng Ren, Rui Men, Dayiheng Liu, Chang Zhou, Jingren Zhou, and Junyang Lin. Qwen2-vl: Enhancing vision-language model’s perception of the world at any resolution. *arXiv preprint arXiv:2409.12191*, 2024. Qwen2.5-VL-3B-Instruct source <https://huggingface.co/Qwen/Qwen2.5-VL-3B-Instruct>.

- [30] Peng Xia, Kangyu Zhu, Haoran Li, Hongtu Zhu, Yun Li, Gang Li, Linjun Zhang, and Huaxiu Yao. RULE: Reliable multimodal rag for factuality in medical vision language models. In *Proceedings of the 2024 Conference on Empirical Methods in Natural Language Processing*, pages 1081–1093, 2024.
- [31] Chong Xiang, Tong Wu, Zexuan Zhong, David Wagner, Danqi Chen, and Prateek Mittal. Certifiably robust RAG against retrieval corruption. *arXiv preprint arXiv:2405.15556*, 2024.
- [32] Jiaqi Xue, Mengxin Zheng, Yebowen Hu, Fei Liu, Xun Chen, and Qian Lou. BadRAG: Identifying vulnerabilities in retrieval augmented generation of large language models. *arXiv preprint arXiv:2406.00083*, 2024.
- [33] Shi Yu, Chaoyue Tang, Bokai Xu, Junbo Cui, Junhao Ran, Yukun Yan, Zhenghao Liu, Shuo Wang, Xu Han, Zhiyuan Liu, et al. Visrag: Vision-based retrieval-augmented generation on multi-modality documents. *arXiv preprint arXiv:2410.10594*, 2024.
- [34] Jianhao Yuan, Shuyang Sun, Daniel Omeiza, Bo Zhao, Paul Newman, Lars Kunze, and Matthew Gadd. Rag-driver: Generalisable driving explanations with retrieval-augmented in-context learning in multi-modal large language model. *arXiv preprint arXiv:2402.10828*, 2024.
- [35] Xin Zhang, Yanzhao Zhang, Wen Xie, Mingxin Li, Ziqi Dai, Dingkun Long, Pengjun Xie, Meishan Zhang, Wenjie Li, and Min Zhang. GME: Improving universal multimodal retrieval by multimodal LLMs. *arXiv preprint arXiv:2412.16855*, 2024.
- [36] Lianmin Zheng, Wei-Lin Chiang, Ying Sheng, Siyuan Zhuang, Zhanghao Wu, Yonghao Zhuang, Zi Lin, Zhuohan Li, Dacheng Li, Eric Xing, et al. Judging llm-as-a-judge with mt-bench and chatbot arena. *Advances in Neural Information Processing Systems*, 36:46595–46623, 2023.
- [37] Huichi Zhou, Kin-Hei Lee, Zhonghao Zhan, Yue Chen, Zhenhao Li, Zhaoyang Wang, Hamed Haddadi, and Emine Yilmaz. Trustrag: Enhancing robustness and trustworthiness in RAG. *arXiv preprint arXiv:2501.00879*, 2025.
- [38] Shengyao Zhuang, Ekaterina Khramtsova, Xueguang Ma, Bevan Koopman, Jimmy Lin, and Guido Zuccon. Document screenshot retrievers are vulnerable to pixel poisoning attacks. *arXiv preprint arXiv:2501.16902*, 2025.
- [39] Wei Zou, Runpeng Geng, Binghui Wang, and Jinyuan Jia. PoisonedRAG: Knowledge corruption attacks to retrieval-augmented generation of large language models. *arXiv preprint arXiv:2402.07867*, 2024.

A Qualitative Attack Examples

We present a qualitative demonstration of our attack against the CLIP-ViT-LARGE embedding model and SmolVLM-Instruct VLM in Figure 2. Despite the success of the attack, the perturbed image is almost indistinguishable from the original.

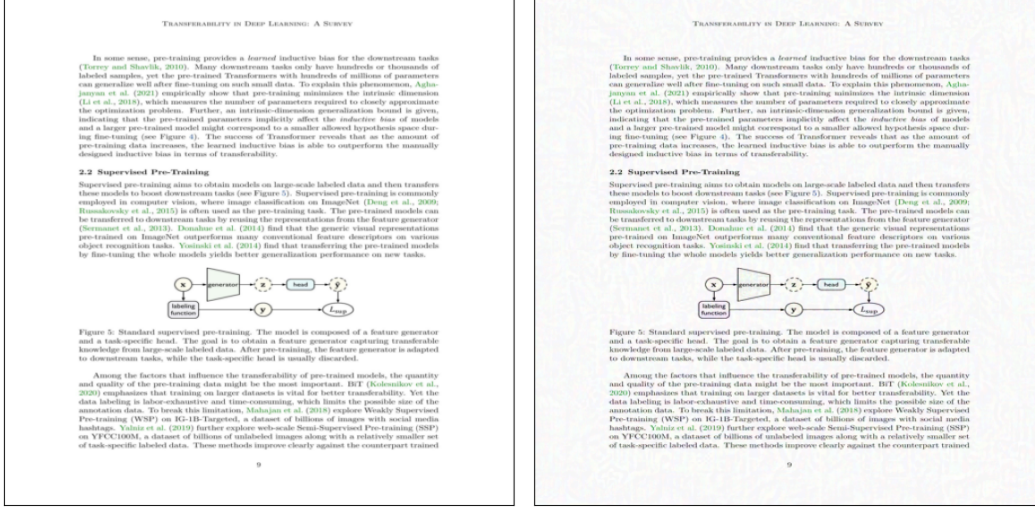


Figure 2: An example of a benign image from the ViDoRe-V1-AI Dataset (left) and its adversarially perturbed counterpart (right). Attack against CLIP-ViT-LARGE, SmolVLM-Instruct, with perturbation intensity $\alpha = \frac{8}{255}$. Result: ASR-R =1, ASR-G-Hard =1.

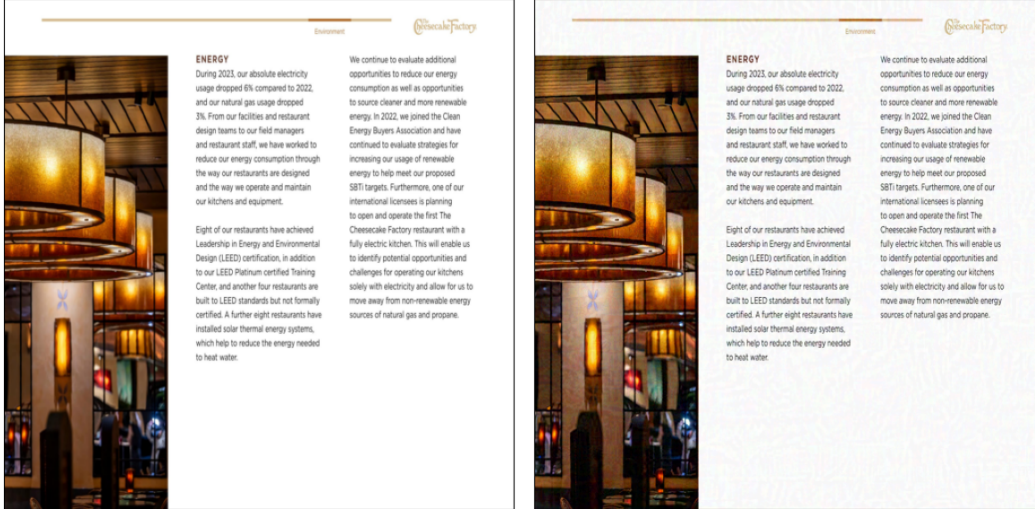


Figure 3: An example of a benign image from the ViDoRe-V2-ESG Dataset (left) and its adversarially perturbed counterpart (right). Attack against CLIP-ViT-LARGE, SmolVLM-Instruct, with perturbation intensity $\alpha = \frac{8}{255}$. Result: ASR-R =0.82, ASR-G-Hard =1.

B Results of the ViDoRe-V2-ESG Dataset

The tables, Table 10 and Table 11, show the universal and targeted attack performance, respectively, for the ViDoRe-V2-ESG dataset.

Table 10: Universal attack against the ESG dataset across different embedding models and VLMs.

Eval Embedder	Eval VLM	Recall-B @1	Recall-A @1	ASR-R @1	Recall-B @5	Recall-A @5	ASR-R @5	ASR-G-Hard @-1	SIM-G-ADV-POS @-1	SIM-G-GT @-1
CLIP-L	SmolVLM	0.134	0.018	0.636	0.360	0.324	0.909	1.000	1.000	0.046
	Qwen2.5-3B	0.134	0.018	0.727	0.360	0.342	0.727	1.000	1.000	0.046
ColPali	SmolVLM	0.519	0.519	0.000	0.826	0.826	0.000	0.636	0.983	0.046
	Qwen2.5-3B	0.519	0.519	0.000	0.826	0.806	0.000	1.000	1.000	0.046
GME	SmolVLM	0.463	0.443	0.000	0.713	0.713	0.091	1.000	1.000	0.046
	Qwen2.5-3B	0.463	0.443	0.000	0.713	0.713	0.091	1.000	1.000	0.046

Table 11: Targeted attacks against the ESG dataset for the different embedding models and VLMs.

Embedder	VLM	ASR-R (@1)	FPR-R (@1)	SIM-G-ADV-POS	SIM-G-ADV-NEG
CLIP-L	SmolVLM	1	0.000	1.000	0.087
	Qwen2.5-3B	1	0.000	0.871	0.105
ColPali	SmolVLM	1	0.000	0.109	0.064
	Qwen2.5-3B	1	0.000	0.044	0.059
GME	SmolVLM	1	0.000	1.000	0.114
	Qwen2.5-3B	1	0.000	0.210	0.142

C Effect of Perturbation Intensity

Figure 4 shows how the maximum adversarial perturbation α affects attack success for a VD-RAG system consisting of CLIP-ViT-LARGE and SmolVLM-Instruct. We observe that attacks can almost perfectly satisfy both the retrieval and the generation conditions starting from $\alpha = \frac{8}{255}$. Therefore, in the rest of the paper, we consider only attacks with $\alpha = \frac{8}{255}$. In Appendix A, we provide visual examples of the stealthiness of an attack with $\alpha = \frac{8}{255}$. The figure also shows very little difference between the performance on the training and test sets, demonstrating that the malicious image does not overfit to the training dataset.

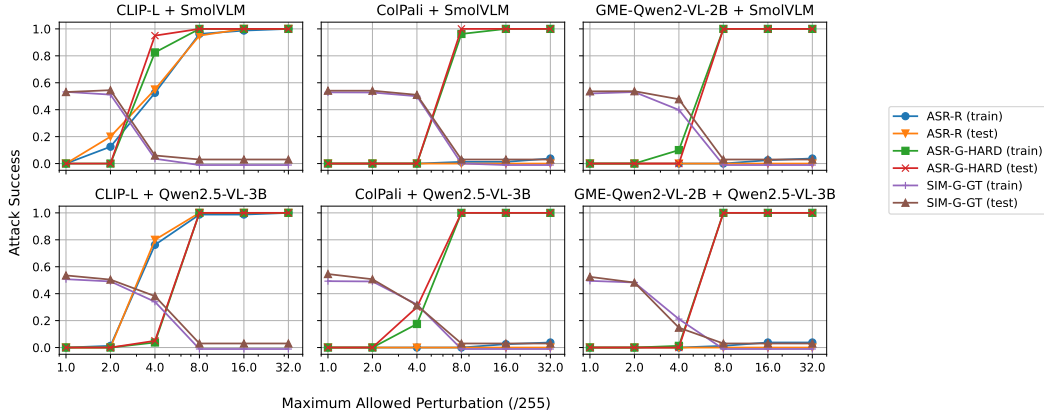


Figure 4: Attack success rate as a function of the perturbation intensity α .

D Black-Box Transferability

The tables, Table 12 and Table 13, show the universal and targeted attack transferability, respectively, for the ViDoRe-V1-AI dataset.

Table 12: Universal attack black-box transferability across embeddings and VLMs.

Train Embedder	Train VLM	Eval Embedder	Eval VLM	ASR-R@1	ASR-R@5	SIM-G-ADV@-1
CLIP-L	SmolVLM	CLIP-L	Qwen2.5-VL-3B	1.000	1.000	-0.020
		ColPali	SmolVLM	0.000	0.000	1.000
		ColPali	Qwen2.5-VL-3B	0.000	0.000	-0.003
		GME-Qwen2-VL-2B	SmolVLM	0.000	0.050	1.000
		GME-Qwen2-VL-2B	Qwen2.5-VL-3B	0.000	0.050	-0.025
CLIP-L	Qwen2.5-VL-3B	CLIP-L	SmolVLM	1.000	1.000	-0.022
		ColPali	SmolVLM	0.000	0.000	-0.033
		ColPali	Qwen2.5-VL-3B	0.000	0.000	1.000
		GME-Qwen2-VL-2B	SmolVLM	0.000	0.000	-0.027
		GME-Qwen2-VL-2B	Qwen2.5-VL-3B	0.000	0.000	1.000
ColPali	SmolVLM	CLIP-L	SmolVLM	0.000	0.000	0.056
		CLIP-L	Qwen2.5-VL-3B	0.000	0.000	-0.003
		ColPali	Qwen2.5-VL-3B	0.000	0.100	-0.024
		GME-Qwen2-VL-2B	SmolVLM	0.000	0.000	0.073
		GME-Qwen2-VL-2B	Qwen2.5-VL-3B	0.000	0.000	-0.004
ColPali	Qwen2.5-VL-3B	CLIP-L	SmolVLM	0.000	0.050	-0.030
		CLIP-L	Qwen2.5-VL-3B	0.000	0.050	1.000
		ColPali	SmolVLM	0.000	0.100	-0.021
		GME-Qwen2-VL-2B	SmolVLM	0.000	0.000	-0.026
		GME-Qwen2-VL-2B	Qwen2.5-VL-3B	0.000	0.000	1.000
GME-Qwen2-VL-2B	SmolVLM	CLIP-L	SmolVLM	0.000	0.000	1.000
		CLIP-L	Qwen2.5-VL-3B	0.000	0.000	-0.001
		ColPali	SmolVLM	0.000	0.000	1.000
		ColPali	Qwen2.5-VL-3B	0.000	0.000	-0.006
		GME-Qwen2-VL-2B	Qwen2.5-VL-3B	0.000	0.250	-0.002
GME-Qwen2-VL-2B	Qwen2.5-VL-3B	CLIP-L	SmolVLM	0.000	0.000	-0.021
		CLIP-L	Qwen2.5-VL-3B	0.000	0.000	1.000
		ColPali	SmolVLM	0.000	0.000	-0.030
		ColPali	Qwen2.5-VL-3B	0.000	0.000	1.000
		GME-Qwen2-VL-2B	SmolVLM	0.000	0.350	-0.028

Table 13: Targeted attack black-box transferability across embeddings and VLMs.

Train Embedder	Train VLM	Eval Embedder	Eval VLM	ASR-R@1	ASR-R@5	SIM-G-ADV@-1
CLIP-L	SmolVLM	CLIP-L	Qwen2.5-VL-3B	0.000	0.000	0.472
		ColPali	SmolVLM	0.000	0.000	1.000
		ColPali	Qwen2.5-VL-3B	0.000	0.000	0.535
		GME-Qwen2-VL-2B	SmolVLM	0.000	0.000	1.000
		GME-Qwen2-VL-2B	Qwen2.5-VL-3B	0.000	0.000	0.446
CLIP-L	Qwen2.5-VL-3B	CLIP-L	SmolVLM	0.000	0.050	0.497
		ColPali	SmolVLM	0.000	0.000	0.602
		ColPali	Qwen2.5-VL-3B	0.000	0.000	1.000
		GME-Qwen2-VL-2B	SmolVLM	0.000	0.000	0.524
		GME-Qwen2-VL-2B	Qwen2.5-VL-3B	0.000	0.000	1.000
ColPali	SmolVLM	CLIP-L	SmolVLM	0.000	0.000	1.000
		CLIP-L	Qwen2.5-VL-3B	0.000	0.000	0.368
		ColPali	Qwen2.5-VL-3B	0.000	0.000	0.481
		GME-Qwen2-VL-2B	SmolVLM	0.000	0.050	1.000
		GME-Qwen2-VL-2B	Qwen2.5-VL-3B	0.000	0.050	0.422
ColPali	Qwen2.5-VL-3B	CLIP-L	SmolVLM	0.000	0.000	0.530
		CLIP-L	Qwen2.5-VL-3B	0.000	0.000	1.000
		ColPali	SmolVLM	0.000	0.000	0.510
		GME-Qwen2-VL-2B	SmolVLM	0.000	0.000	0.508
		GME-Qwen2-VL-2B	Qwen2.5-VL-3B	0.000	0.000	1.000
GME-Qwen2-VL-2B	SmolVLM	CLIP-L	SmolVLM	0.000	0.000	1.000
		CLIP-L	Qwen2.5-VL-3B	0.000	0.000	0.401
		ColPali	SmolVLM	0.000	0.000	1.000
		ColPali	Qwen2.5-VL-3B	0.000	0.000	0.529
		GME-Qwen2-VL-2B	Qwen2.5-VL-3B	0.000	0.000	0.537
GME-Qwen2-VL-2B	Qwen2.5-VL-3B	CLIP-L	SmolVLM	0.000	0.000	0.497
		CLIP-L	Qwen2.5-VL-3B	0.000	0.000	0.998
		ColPali	SmolVLM	0.000	0.000	0.497
		ColPali	Qwen2.5-VL-3B	0.000	0.000	1.000
		GME-Qwen2-VL-2B	SmolVLM	0.000	0.000	0.534

E Embedding Space Visualizations

In this section, we present two-dimensional UMAP visualizations [23] of the embeddings for images and user queries, employing the models CLIP-ViT-LARGE, ColPali-v1.3, and GME-Qwen2-VL-2B, and using the first 100 samples from `vidore/syntheticDocQA_artificial_intelligence_test` [7]. The visualizations are depicted in Figures 5, 6, and 7, respectively. Notably, while CLIP-ViT-LARGE and GME-Qwen2-VL-2B produce a single normalized vector embedding for each image or query, ColPali-v1.3 generates one normalized vector embedding per token, resulting in multiple vectors for each query and image. To effectively represent each query and image as a singular point within the same UMAP coordinate space, we adopt a symmetrized and normalized late interaction (MaxSim) distance metric for the UMAP visualization, defined as

$$\text{LI}_{NS}(Q, I) = \frac{1}{2} \times \text{LI} \left(\frac{Q}{|Q|}, I \right) + \frac{1}{2} \times \text{LI} \left(\frac{I}{|I|}, Q \right), \quad (4)$$

where Q and I are the sets of query and image embeddings generated by a query q and an image i , respectively, and LI is the late interaction [7] defined as,

$$\text{LI}(Q, I) = \sum_{i \in [1, N_Q]} \max_{j \in [1, N_I]} \langle E_Q^i | E_I^j \rangle, \quad (5)$$

where N_Q and N_I are the number of vector embeddings in Q and I , and E_Q^i , and E_I^j represent these embeddings indexed by i and j .

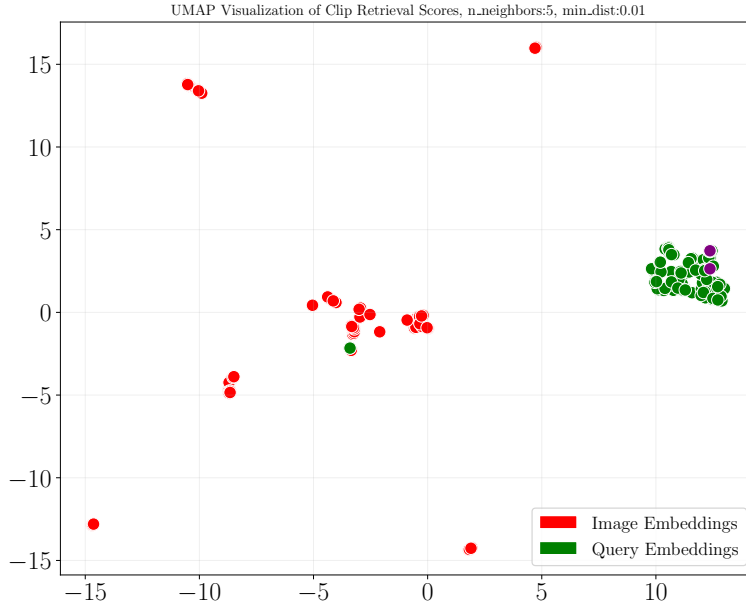


Figure 5: UMAP visualization of the embeddings generated by CLIP-ViT-LARGE

The figures show that, within the low-dimensional UMAP space, the image and text embeddings generated by CLIP-ViT-LARGE are distinctly clustered, whereas those produced by ColPali-v1.3 and GME-Qwen2-VL-2B do not exhibit clear clusters corresponding to queries and images. This distinction might explain why it is feasible to attack the CLIP-ViT-LARGE model. It is possible to create an artificial image that closely aligns with all queries, as its embeddings cluster in the same region. In Figure 5, we show such artificial attack images as purple circles. On the other hand, the

ColPali-v1.3 and GME-Qwen2-VL-2B models lack a consolidated area that encompasses all queries, making it difficult, if not impossible, to generate an image that is in close proximity to all queries.

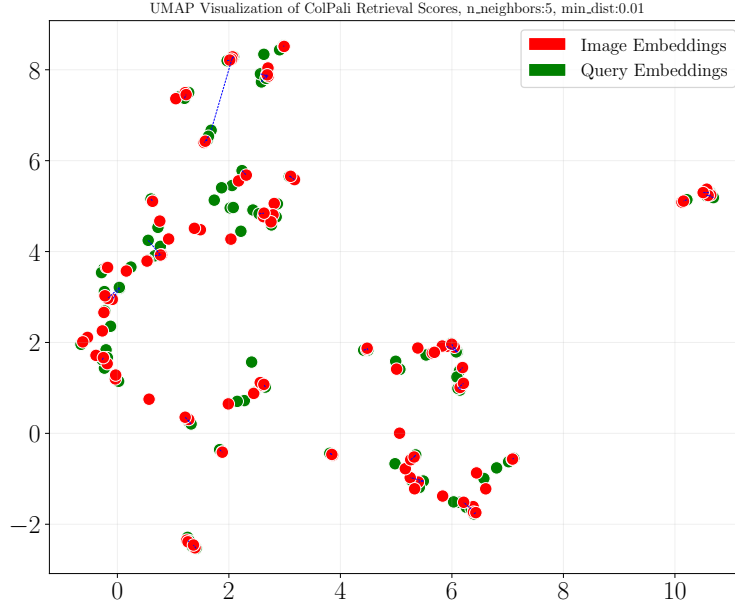


Figure 6: UMAP visualization of the embeddings generated by ColPali-v1.3

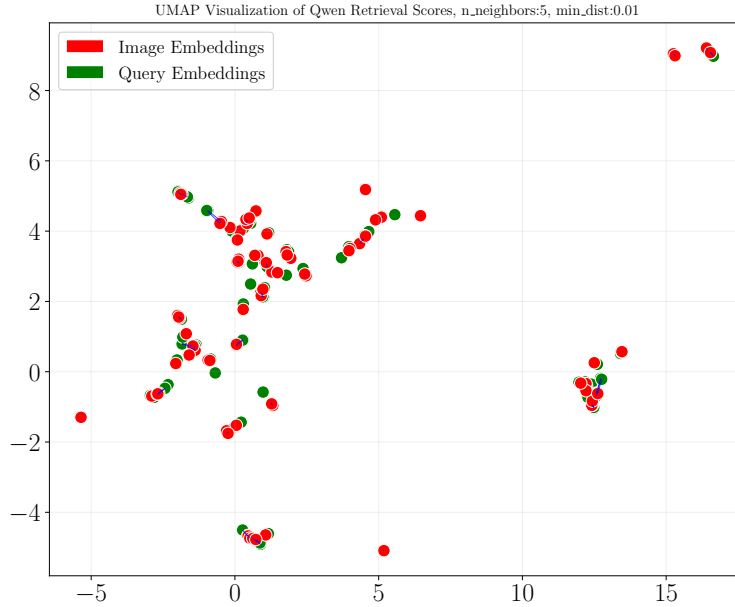


Figure 7: UMAP visualization of the embeddings generated by GME-Qwen2-VL-2B

Additionally, in Figures 6 and 7, using blue dashed lines, we highlight the query-image pairs where the nearest neighbor of the query does not correspond to its true ground truth image. We find that such pairs are quite rare, and even when they do occur, they are typically situated close to each other within their respective clusters. This observation may provide insights into why models like ColPali-v1.3 and GME-Qwen2-VL-2B outperform models like CLIP-ViT-LARGE in retrieval tasks.

F Multi-Model Generalization

The tables, Table 14 and Table 15, show the universal and targeted attack generalizability when trained on multiple models, respectively, for the ViDoRe-V1-AI dataset.

Table 14: Universal attack generation performance across evaluation-time embedding and VLM configurations for two attack settings (recall metrics removed).

Attack Type	Eval Embedder	Eval VLM	ASR-R@1	ASR-R@5	ASR-G-HARD@-1	SIM-G-ADV@-1	SIM-G-GT@-1
2x2 Attack	CLIP-L	SmolVLM	0.900	1.000	0.950	0.952	0.046
		Qwen2.5-VL-3B	0.900	1.000	1.000	1.000	0.030
	GME-Qwen2-VL-2B	SmolVLM	0.000	0.250	1.000	1.000	0.030
		Qwen2.5-VL-3B	0.000	0.250	1.000	1.000	0.030
3x2 Attack	CLIP-L	SmolVLM	0.250	0.700	0.550	0.603	0.207
		Qwen2.5-VL-3B	0.250	0.700	0.950	0.966	0.042
	ColPali	SmolVLM	0.000	0.000	0.550	0.637	0.142
		Qwen2.5-VL-3B	0.000	0.000	0.950	0.994	0.033
	GME-Qwen2-VL-2B	SmolVLM	0.000	0.050	0.600	0.664	0.197
		Qwen2.5-VL-3B	0.000	0.050	1.000	1.000	0.030

Table 15: Performance of targeted attacks jointly computed against multiple embedders and VLMs.

Attack Type	Eval Embedder	Eval VLM	ASR-R @1	FPR-R @1	ASR-R @5	FPR-R @5	SIM-G-ADV-POS	SIM-G-ADV-NEG
2x2 Attack	CLIP-L	SmolVLM	1.000	0.000	1.000	0.050	1.000	-0.003
		Qwen2.5-3B	1.000	0.000	1.000	0.050	1.000	0.027
	GME	SmolVLM	1.000	0.000	1.000	0.000	1.000	-0.011
		Qwen2.5-3B	1.000	0.000	1.000	0.000	1.000	0.044
3x2 Attack	CLIP-L	SmolVLM	1.000	0.000	1.000	0.000	1.000	-0.008
		Qwen2.5-3B	1.000	0.000	1.000	0.000	1.000	0.157
	ColPali	SmolVLM	1.000	0.000	1.000	0.000	0.048	-0.019
		Qwen2.5-3B	1.000	0.000	1.000	0.000	1.000	0.223
	GME	SmolVLM	0.000	0.000	1.000	0.000	0.014	-0.010
		Qwen2.5-3B	0.000	0.000	1.000	0.000	1.000	0.362

G Judge Prompts

The following details the utilized prompts for the VLM-as-a-Judge defense.

Answer Relevancy Prompt. *"Evaluate the following metric: answer_relevancy: Is the answer relevant to the user's query? (YES or NO) QUERY: »query« ANSWER: »answer« Write out in a step by step manner your reasoning to be sure that your conclusion is correct by filling out the following JSON format with the grade and a concise reason behind the grade: grade: ' ', 'reason': ' ' Output the reason as a string, not as a list. The only allowed grades are YES or NO."*

Image Context Relevancy Prompt. *"Evaluate the following metric by comparing the user query with the provided image: image_context_relevancy: Is the content of the images relevant to the user's query, i.e. can it contribute to answer the query? (YES or NO) QUERY: »query« IMAGES: »images« Write out in a step by step manner your reasoning to be sure that your conclusion is correct by filling out the following JSON format with the grade and a concise reason behind the grade: grade: ' ', 'reason': ' ' Output the reason as a string, not as a list. The only allowed grades are YES or NO."*

Image Faithfulness Prompt. *"Evaluate the following metric by comparing the answer with the provided images: image_faithfulness: Is the answer faithful to the content of the images, i.e. does it factually align with any of the images? (YES or NO) GENERATED ANSWER: »answer« IMAGES: »images« Write out in a step by step manner your reasoning to be sure that your conclusion is correct by filling out the following JSON format with the grade and a concise reason behind the grade: grade: ' ', 'reason': ' ' Output the reason as a string, not as a list. The only allowed grades are YES or NO."*

H Limitations

Since we only inject one image into the KB, our attacks can be easily detected by majority vote-based [31] methods. However, these methods often increase the latency of the system, and might degrade the benign performance. Moreover, we could not evaluate our attacks against very large embedding models and VLMs due to compute constraints.

I Societal Impact

The authors acknowledge the potential for misuse of this work through the creation of malicious inputs for AI systems. However, the authors believe that VD-RAG is a developing technology and therefore evaluating the robustness of the proposed approaches is critical to evaluating risks and mitigating them. Therefore, we hope that the results presented in this work will aid in the development of defenses for and the safe design of future VD-RAG systems.